Saudi Journal of Biological Sciences 26 (2019) 808–815

Contents lists available at ScienceDirect

Saudi Journal of Biological Sciences

journal homepage: www.sciencedirect.com

Original article

Pyrolysis molecule of *Torreya grandis* bark for potential biomedicine

Huiling Chen [a,1], Xiaochen Yue [a,1], Jun Yang [a,1], Chunxia Lv [b,1], Shuaiwei Dong [b,1], Xuefeng Luo [b], Zhiyong Sun [b], Ying Zhang [b], Baoxiang Li [b], Faping Zhang [b], Haiping Gu [a,*], Yafeng Yang [a,*], Qiuling Zhang [a,*], Shengbo Ge [c,*], Huitao Bi [a,*], Dongfang Zheng [a,*], Yong Zhao [a,*], Cheng Li [a,*], Wanxi Peng [a,*]

[a] School of Forestry, Henan Agricultural University, Zhengzhou 450002, China
[b] The Scientific Research Institution, Henan Xiaoqinling National Nature Reserve Administration Bureau, Sanmenxia 472500, China
[c] Department of Mechanical and Energy Engineering, University of North Texas, Denton, TX 76203, USA

ARTICLE INFO

Article history:
Received 11 December 2018
Revised 7 January 2019
Accepted 8 January 2019
Available online 9 January 2019

Keywords:
Torreya grandis bark
TG
Py-GC/MS

ABSTRACT

Torreya grandis is a unique tree species in China. Although full use has been made of the timber, the processing and utilization of the bark has not been effective. In order to explore a new way to utilize the bark of *Torreya grandis*, a powder of *T. grandis* bark was prepared and analyzed qualitatively and quantitatively. Differential scanning calorimetry (TG) and pyrolysis gas chromatography-mass spectrometry (PY-GC/MS) revealed many bioactive components in the bark of *T. grandis, such* as acetic acid, 2-methoxy-4-vinyl phenol, D-mannose, and furfural. These substances have potential broad applications in the chemical industry, biomedicine, and food additives. The chemical constituents of the bark of T. grandis suggest a theoretical basis for the future development and utilization of the bark of *T. grandis*.

1. Introduction

The tree *Torreya grandis* grows as high as 25 m, with a diameter at breast height of 65 cm, and is mainly found in southern Jiangsu, Zhejiang, northern Fujian, southern Anhui and Dabie Mountains, Northwestern Jiangsu, and other mountains below 1400 m in altitude (Zhu et al., 2015). In the valley of the shade, the trees grow well, due to a warm and humid environment, with winter temperature of −15 °C without freezing damage (Li et al., 2014). The tree grow for 200 years old, it is usually propagated with seeds, with a high germination rate, generally up to 80% (Zeng et al., 2014).

Meanwhile Torreya seeds can be used to make oil, edible oil, lubricants, and wax. The acetic acid linaloid and rose oil contained in Torreya seeds are raw materials for the refinement of high-grade aromatic oil (Ni and Shi, 2014; Shi et al., 2009). The Torreya tree has a neat crown and rich foliage (Liu, 2018; Zong et al., 2018). Big trees are planted alone as shade trees at the edge of lawn, or around buildings. They have strong anti-pollution ability and adapt to the urban ecological environment. They are widely used in greening, industrial areas, and have high economic value (Saeed et al., 2010; Chen et al., 2006). Torreya bark is pale yellow gray, dark gray, or grayish brown, with irregular longitudinal cracks. It is thick skinned on the outside layer of the tree (Wang et al., 2002).

Torreya grandis is an endemic tree in China, and its wood has many functions. Due to the lack of development and utilization of high value-added products, most *T. grandis* bark is used as firewood. We extracted the *T. grandis* bark as powder. Differential scanning calorimetry (TG) and pyrolysis gas chromatography-mass spectrometry (PY-GC/MS) were used to study the pyrolysis reaction of the bark of *Torreya grandis* during heating and the types of high temperature catalytic cracking products in order to provide a new method for the utilization of high-grade resources of Chinese *Torreya* bark.

2. Material and methods

2.1. Experimental materials

Torreya samples were collected from the Xixia Forest District in Henan Province. The bark was processed into powder of 40–60 meshes by a pulverizer, followed by baking at 55 °C under a vacuum of 0.01 MPa to dryness for use (Wang et al., 2018).

* Corresponding authors.
E-mail address: pengwanxi@163.com (W. Peng).
[1] Co-first authors.
Peer review under responsibility of King Saud University.

Production and hosting by Elsevier

https://doi.org/10.1016/j.sjbs.2019.01.005
1319-562X/

2.2. TG analysis

The *Torreya grandis* bark was analyzed by thermogravimetry (TGA Q50 V20.8 Build 34). The nitrogen release rate was 60 mL/min. The temperature program of TG started at 30 °C and rose to 300 °C at a rate of 5 °C/min (Duan et al., 2018).

2.3. Py-GC/MS analysis

Py-gas chromatography (GC)/mass spectrometry (MS) triple system, Py using Frontier's PY-2020iS cracker, GC/MS Agilent 5975C/6890N GC–MS (Ge et al., 2017; Li et al., 2015). Gas chromatography conditions: The column was a DB-5 MS (30 m × 0.25 mm × 0.25 μm) elastic silica capillary column manufactured by Agilent Company (Peng et al., 2017). The carrier gas was helium, inlet temperature is 250 °C; column ascending conditions: 50–300 °C at 10 °C/min, 30:1 split injection (Peng et al., 2016a, 2016b). Mass spectrometry conditions: ionization mode EI, electron energy 70 eV, He flow rate 1 mL/min, scanning mass range 35–550 AMU (*m*/*z*) (Peng et al., 2016a, 2016b).

3. Results and analysis

3.1. Behavior of the Torreya grandis bark during heating

In order to study the thermal decomposition of the bark of *Torreya grandis*, we conducted a TGA test on the samples (Fig. 1). The TGA analysis of the bark of *Torreya grandis* revealed that the weightlessness process of pyrolysis process can be divided into three stages. The first stage is the evaporation stage of water, which is 23–90 °C. At this stage, the weight loss of the sample is very small, and may be caused by the loss of moisture in the sample (Debbarma et al., 2018). The second stage is between 90 °C and 175 °C, which is the transition phase of the preheating solution. The differential curve of this stage is relatively flat, indicating that the pyrolysis rate is relatively stable, and the sample begins to show obvious weight loss (Lans and Vodovotz, 2018). Weightlessness is mainly due to a small amount of polymer depolymerization and recombination in the sample. The third stage is between 175 °C and 300 °C. *Torreya grandis* bark rapidly decomposes and produces a large amount of volatile gas, resulting in weightlessness (Raba et al., 2018). The three stages have different kinetic parameters and reaction mechanisms, and the final bark residual mass of *T. grandis* is 76.29%. During the whole process, the bark heat weight of *Torreya grandis* was only about 23%, the weight loss was small, the mass change was small, and the speed was low. The thermal decomposition process of the bark of *Torreya grandis* under 300 °C was analyzed by TG experiment, which provided a reference for the thermal decomposition of the bark of *Torreya grandis* under certain conditions. That is to say, in order to ensure that the organic matter content in the bark of *Torreya grandis* does not lose much during heat treatment, the temperature should be controlled below 90 °C in order to make full use of the bark of *Torreya grandis* (Wu et al., 2018).

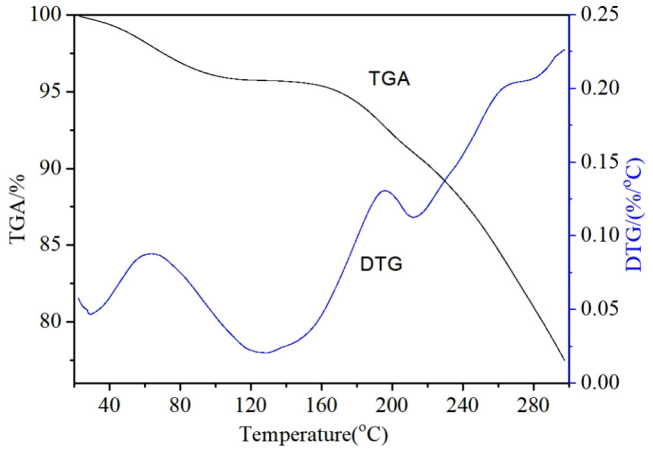

Fig. 1. TGA and DTG thermal curves of *Torreya grandis* bark.

3.2. Identification of pyrolysis products of Torreya grandis bark

For further study, PY-GC/MS experiments were carried out. Under the above experimental conditions, the pyrolysis gas of *Torreya grandis* bark was analyzed by on-line GS/MS (Francisco et al., 2011). The chromatographic ion chromatogram and mass spectrometry data were obtained (Fig. 2). Based on the total ion current plot, the microprocessor configured by GC–MS used area normalization to calculate the relative percentages of peak areas (Vielhauer et al., 2011; Mehrabian et al., 2015). The NIST standard library was used to search mass spectrometry data automatically of each peak by electronic computer (Lin et al., 2018; Okamoto et al., 2018). The chromatograms of each peak were compared with manual spectrum analysis and the published relevant mass spectrometry data (Kim et al., 2018a, 2018b). *Torreya grandis* bark pyrolysis products of the main chemical composition were compared (Fang et al., 2018). 225 peaks were found in the gas chromatogram of pyrolysis products, which were analyzed by MS and literature review, 205 compounds were identified (Table 1). Some of these substances were analysed briefly below.

Acetone (3.12%) is an important raw material for organic synthesis, used in the production of epoxy resin, polycarbonate, plexiglass, and other solvents, and used as extractant and diluent (Zhang et al., 2018a, 2018b). In the pharmaceutical industry, it is one of the raw materials of vitamin C and anesthetic sophora, and is also used as a vitamin and hormone production process extractant. Acetone is one of the raw materials for the synthesis of pyrethroid in pesticide industry (Fedorovich et al., 2018; Yang et al., 2018).

2, 3-Butanedione (0.49%) is mainly used to make food flavors (Kastier et al., 2018). It is the main flavor of cream, and can also

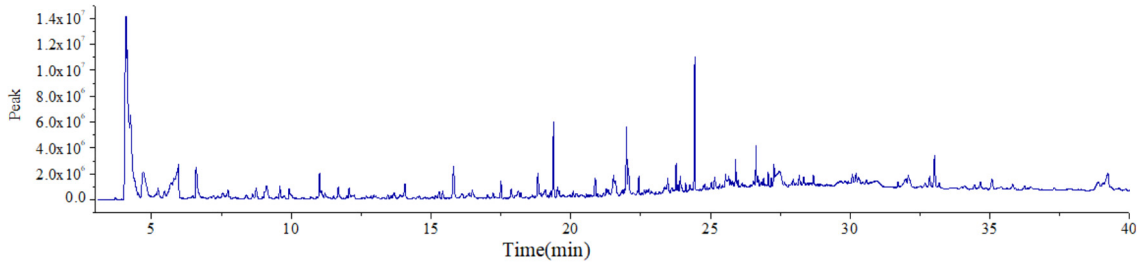

Fig. 2. Total ion current plot of pyrolyzed product of *Torreya grandis* Bark.

Table 1
Torreya grandis Bark pyrolysis products identification table.

No.	Retention time (min)	Relative content (%)	Compounds name
1	3.71	0.06	2-Propenamide
2	4.09	14.86	Ethyne, fluoro-
3	4.25	6.37	Carbon dioxide
4	4.54	0.22	Methylamine, N,N-dimethyl-
5	4.70	3.12	Acetone
6	5.13	0.10	2-Propen-1-ol
7	5.20	0.21	2-Propen-1-ol, 2-methyl-
8	5.24	0.54	Acetaldehyde, hydroxy-
9	5.46	0.49	2,3-Butanedione
10	5.70	1.56	Furan, 2-methyl-
11	5.80	0.93	Acetic acid
12	5.98	2.72	Acetic acid
13	6.47	0.35	Butanal, 3-methyl-
14	6.60	1.83	2-Propanone, 1-hydroxy-
15	7.10	0.16	Acetic acid, sodium salt
16	7.21	0.23	Heptane
17	7.39	0.22	1,2-Ethanediol
18	7.55	0.41	Furan, 2,5-dimethyl-
19	7.74	0.53	Propanoic acid
20	7.95	0.07	3-Methylpyridazine
21	8.01	0.08	Butyric acid hydrazide
22	8.40	0.26	1H-Pyrrole, 1-methyl-
23	8.61	0.21	Pyridine
24	8.75	0.52	Pyrrole
25	8.98	0.06	Butanenitrile, 2,3-dioxo-, dioxime, O,O'-diacetyl-
26	9.06	0.17	2-Propanone, 1-hydroxy-
27	9.12	0.82	Toluene
28	9.46	0.16	Acetylacetone
29	9.60	0.46	Propanoic acid, 2-oxo-, methyl ester
30	9.76	0.20	1,2-Cyclopentanediol, trans-
31	9.93	0.58	3-Amino-s-triazole
32	10.39	0.05	3-Furaldehyde
33	10.46	0.06	Methanesulfonic acid, methyl ester
34	10.71	0.09	Ethanol, 2-[(2-aminoethyl)amino]-
35	10.76	0.07	4-Aminopyridine
36	10.92	0.07	Butanenitrile, 4-oxo-
37	11.02	0.76	Furfural
38	11.08	0.34	2-Cyclopenten-1-one
39	11.22	0.23	1H-Pyrrole, 3-methyl-
40	11.52	0.11	1H-Pyrrole, 3-methyl-
41	11.69	0.43	2-Furanmethanol
42	12.00	0.11	Ethylbenzene
43	12.08	0.33	2-Propanone, 1-(acetyloxy)-
44	12.19	0.15	1,2-Cyclopentanedione
45	12.25	0.14	p-Xylene
46	12.69	0.13	4-Cyclopentene-1,3-dione
47	12.86	0.08	1-Nonene
48	12.96	0.14	Bicyclo [4.2.0]octa-1,3,5-triene
49	13.04	0.11	Propanedioic acid, propyl-
50	13.46	0.12	2-Cyclopenten-1-one, 2-methyl-
51	13.58	0.12	Ethanone, 1-(2-furanyl)-
52	13.68	0.34	2(5H)-Furanone
53	13.90	0.24	Hexane, 3,3,4-trimethyl-
54	14.08	0.65	2-Cyclopenten-1-one, 2-hydroxy-
55	14.52	0.07	2(5H)-Furanone, 5-methyl-
56	14.58	0.09	2,5-Furandione, 3-methyl-
57	14.79	0.07	Dihydro-3-methylene-5-methyl-2-furanone
58	15.05	0.08	Pentanoic acid, 4-methyl-
59	15.17	0.13	*trans*-1-Ethoxy-1-butene
60	15.30	0.29	2-Furancarboxaldehyde, 5-methyl-
61	15.42	0.25	2-Cyclopenten-1-one, 3-methyl-
62	15.82	1.23	Phenol
63	16.11	0.19	Heptanoic acid
64	16.14	0.07	1-Decene
65	16.28	0.04	Glycerin
66	16.31	0.03	Diglycerol
67	16.36	0.16	1H-1,2,4-Triazol-3-amine, 1-ethyl-
68	16.48	0.23	2-Methyliminoperhydro-1,3-oxazine
69	17.04	0.11	4(1H)-Pyrimidinone, 6-hydroxy-
70	17.22	0.17	2-Cyclohexen-1-one
71	17.32	0.09	Hexane, 2,5-dimethyl-
72	17.51	0.48	2-Cyclopenten-1-one, 2-hydroxy-3-methyl-
73	17.88	0.33	2-Cyclopenten-1-one, 2,3-dimethyl-

Table 1 (*continued*)

No.	Retention time (min)	Relative content (%)	Compounds name
74	18.14	0.52	1,3-Dioxol-2-one,4,5-dimethyl-
75	18.22	0.15	Phenol, 2-methyl-
76	18.40	0.09	Benzene, n-butyl-
77	18.64	0.09	Furaneol
78	18.74	0.06	Acetophenone
79	18.83	0.87	p-Cresol
80	18.94	0.18	6-Heptenoic acid
81	19.01	0.13	Heptanoic acid
82	19.10	0.41	Heptanoic acid
83	19.20	0.09	Furyl hydroxymethyl ketone
84	19.29	0.19	3-Acetoxydodecane
85	19.39	1.98	Phenol, 2-methoxy-
86	19.54	0.34	2-Butanamine, 3-methyl-
87	19.60	0.19	Furan, 2-methyl-
88	19.73	0.20	1-Cyclopropanecarbonitrile, 1-amino
89	19.97	0.22	Benzofuran, 2-methyl-
90	20.09	0.18	Maltol
91	20.20	0.14	2H-Pyran-3(4H)-one, dihydro-6-methyl-
92	20.24	0.09	2-Cyclopenten-1-one, 3-ethyl-2-hydroxy-
93	20.38	0.17	2-Pentenoic acid, 4-hydroxy-
94	20.57	0.08	Phenol, 3-ethyl-
95	20.64	0.05	2-Propanamine, N-methyl-N-nitroso-
96	20.72	0.07	Benzyl nitrile
97	20.88	0.63	4H-Pyran-4-one, 2,3-dihydro-3,5-dihydroxy-6-methyl-
98	20.97	0.08	2H-Pyran-2-one, tetrahydro-
99	21.06	0.04	Cycloprop[a]indene, 1,1a,6,6a-tetrahydro-
100	21.18	0.14	1-Methyl-3-piperidinemethanol
101	21.28	0.18	Phenol, 4-ethyl-
102	21.35	0.28	Cyclopentane, 2-methyl-1-methylene-3-(1-methylethenyl)-
103	21.41	0.08	2-Isopropyl-3-methoxycyclopropanecarboxylic acid, methyl ester
104	21.54	0.86	Octanoic acid, silver(1 +) salt
105	21.58	0.82	1,3-Dioxane-5-methanol, 5-ethyl-
106	21.82	0.13	Cyclododecane
107	21.87	0.16	4-Hydroxy-N-methylpiperidine
108	21.94	0.17	4H-Pyran-4-one, 3,5-dihydroxy-2-methyl-
109	22.00	1.54	Creosol
110	22.06	1.22	Catechol
111	22.39	0.11	1,4:3,6-Dianhydro-.alpha.-d-glucopyranose
112	22.44	0.42	Benzofuran, 2,3-dihydro-
113	22.54	0.06	1H-Benzimidazole, 2-ethyl-
114	22.63	0.14	m-Guaiacol
115	22.71	0.17	5-Hydroxymethylfurfural
116	22.79	0.19	2,6,10-Dodecatrien-1-ol, 3,7,11-trimethyl-, (Z,E)-
117	22.89	0.11	Cyclopentan-1-al, 4-isopropylidene-2-methyl-
118	23.04	0.06	Benzylidene-l-ornithine
119	23.18	0.07	Phenol, 4-(2-propenyl)-
120	23.26	0.05	1,3-Cyclopentadiene, 5,5-dimethyl-2-propyl-
121	23.35	0.18	*trans*-2-Dodecen-1-ol, trifluoroacetate
122	23.38	0.23	1,2-Benzenediol, 3-methyl-
123	23.47	0.59	1,2-Benzenediol, 3-methoxy-
124	23.62	0.27	Hydroquinone
125	23.71	0.10	1-(Dimethylamino)pyrrole
126	23.77	0.66	Phenol, 4-ethyl-2-methoxy-
127	23.84	0.23	1-Tridecene
128	23.93	0.55	1,2-Benzenediol, 4-methyl-
129	23.98	0.18	Tridecane
130	24.12	0.28	Indole
131	24.26	0.39	2-Allylphenol
132	24.34	0.13	2,6-Octadiene, 2,6-dimethyl-
133	24.44	2.98	2-Methoxy-4-vinylphenol
134	24.64	0.12	1,4-Benzenediol, 2-methyl-
135	24.76	0.26	Biphenylene, 1,2,3,6,7,8,8a,8b-octahydro-, trans-
136	24.79	0.21	Phenol, 4-(2-propenyl)-
137	24.88	0.16	2,4-Diaminophenol
138	24.96	0.11	N-(2,6-Dimethyl-phenyl)-2-(2-methyl-5-nitro-imidazol-1-yl)-acetamide
139	25.04	0.44	9-Decenoic acid
140	25.16	0.48	Eugenol
141	25.20	0.15	Hexyl 8-methylnon-6-enoate
142	25.26	0.14	(6R)-7a-Hydroxy-3,6-dimethyl-5,6,7,7a-tetrahydrobenzofuran-2(4H)-one
143	25.33	0.26	Phenol, 2-methoxy-4-(methoxymethyl)-
144	25.43	0.25	1H-Indene, 2-butyl-5-hexyloctahydro-
145	25.54	0.75	1-Tetradecene
146	25.66	0.69	3,4-Altrosan
147	25.73	0.35	Indole, 3-methyl-

(*continued on next page*)

Table 1 (*continued*)

No.	Retention time (min)	Relative content (%)	Compounds name
148	25.80	0.36	1,4-Benzenediol, 2-methoxy-
149	25.90	0.95	Vanillin
150	25.99	0.26	*trans*-Isoeugenol
151	26.13	0.33	Benzoic acid, 3-hydroxy-, methyl ester
152	26.18	0.17	4′'a-Methyl-8′'-methylidene-decahydro-2′'H-dispiro[bis(cyclopropane)-1,1′:2′,1′'-naphtho[2,3-b]furan]-2′'-one
153	26.24	0.25	Cyclopentanol, 2-cyclopentylidene-
154	26.44	0.21	Benzenemethanol, alpha.,4-dimethyl-
155	26.54	0.44	Z,Z-2,13-Octadecadien-1-ol
156	26.63	1.09	*trans*-Isoeugenol
157	26.71	0.41	E-9-Tetradecenoic acid
158	26.83	0.39	2-Isopropyl-5,6-dimethyl-1,3-oxathiane
159	26.90	0.33	1,5-Dodecadiene
160	26.97	0.21	1,5-Dodecadiene
161	27.07	0.45	1-Octadecene
162	27.18	0.27	Pentadecane
163	27.28	0.76	Apocynin
164	27.41	1.03	.beta.-D-Glucopyranose, 1,6-anhydro-
165	27.47	1.56	.beta.-D-Glucopyranose, 1,6-anhydro-
166	27.66	0.21	2(1H)-Pyridinethione, 1-ethenyl-
167	27.83	0.14	*cis*-Vaccenic acid
168	27.89	0.20	2-Furanmethanamine
169	27.97	0.28	2-Propanone, 1-(4-hydroxy-3-methoxyphenyl)-
170	28.07	0.17	(1-Methoxy-1-methylbut-2-enyl)benzene
171	28.18	0.42	Dodecanoic acid
172	28.25	0.20	Oleic Acid
173	28.33	0.45	2,4,6-Cycloheptatrien-1-one, 2-hydroxy-5-(1-methylethyl)-
174	28.46	0.17	4-Methyl-2,5-dimethoxybenzaldehyde
175	28.52	0.14	4(1H)-Isobenzofuranone, hexahydro-3a,7a-dimethyl-, cis-(.+/-.)-
176	28.58	0.12	1,5-Dodecadiene
177	28.61	0.10	5-Butyl-1,3-oxathiolan-2-one
178	28.69	0.44	Cetene
179	28.81	0.08	1-Chloroeicosane
180	28.86	0.10	10-Methyltricyclo[4.3.1.1(2,5)]undecan-10-ol
181	28.94	0.12	Cyclohexane, (3-chloro-1-propynyl)-
182	29.16	0.09	3-Penten-2-one, 3-bromo-4-methyl-
183	29.55	0.21	n-Hexadecanoic acid
184	29.65	0.33	Melezitose
185	29.70	0.14	Estra-1,3,5(10)-trien-17.beta.-ol
186	29.81	0.32	Estra-1,3,5(10)-trien-17.beta.-ol
187	29.93	0.17	n-Hexadecanoic acid
188	30.08	0.52	Benzenepropanol, 4-hydroxy-3-methoxy-
189	30.21	0.50	6-*tert*-Butyl-2,4-dimethylphenol
190	30.30	0.46	1-(5-Dimethylethyl)pyrazin-2-yl-ethan-1-one
191	30.44	0.09	2- Chloropropionic acid, hexadecyl ester
192	30.59	0.26	1-Heptadecene
193	30.74	0.14	2-Hydroxy-1,1,10-trimethyl-6,9-epidioxydecalin
194	30.81	0.06	Decanoic acid, 3-methyl-
195	30.86	0.11	2-Trimethylsilyl-1,3-dithiane
196	30.95	0.32	*tert*-Butyldimethylsilyl 23-acetoxy-3,6,9,12,15,18,21-heptaoxatricosan-1-oate
197	31.71	0.19	Thiazolo[5,4-f]quinoline
198	31.98	0.72	.beta.-(4-Hydroxy-3-methoxyphenyl)propionic acid
199	32.09	0.54	4-((1E)-3-Hydroxy-1-propenyl)-2-methoxyphenol
200	32.14	0.25	Tetradecanoic acid
201	32.51	0.08	1H-Pyrazole-4-carbaldehyde, 3-(3-hydroxyphenyl)-
202	32.68	0.28	9-Eicosene, (E)-
203	32.85	0.48	9-Octadecen-1-ol, (E)-
204	33.02	1.12	1-Octadecene
205	33.19	0.18	Octadecane
206	33.98	0.11	10-Methyltricyclo[4.3.1.1(2,5)]undecan-10-ol
207	34.09	0.23	4-Hydroxy-7-methyl-pyrano[4,3-b]pyran-2,5-dione
208	34.44	0.21	Cyclohexanone, 2,2-dimethyl-5-(3-methyloxiranyl)-, [2.alpha.(R*),3.alpha.]-(. + -.)-
209	34.66	0.46	5-(4-Methoxyphenyl)thiazol-2-ylamine
210	34.86	0.12	Cyclopentadecanone, 2-hydroxy-
211	35.08	0.50	Pentadecanoic acid
212	35.32	0.07	Octadecanoic acid
213	35.39	0.06	Octadecanoic acid
214	35.82	0.17	Cyclotetradecane
215	36.24	0.18	1-Octadecene
216	36.36	0.05	Pyrimidine-5-carbonitrile, 3,4-dihydro-6-(dimethylaminophenyl)-2-mercapto-4-oxo-
217	36.47	0.14	Octadecane, 1-chloro-
218	37.30	0.11	9-Hexadecenoic acid, methyl ester, (Z)-
219	38.89	0.87	Hexadecenoic acid, Z-11-
220	39.04	0.47	Cyclopentadecanone, 2-hydroxy-

Table 1 (*continued*)

No.	Retention time (min)	Relative content (%)	Compounds name
221	39.22	1.53	n-Hexadecanoic acid
222	39.62	0.17	Dibutyl phthalate
223	39.86	0.09	Cyclopentadecanone, 2-hydroxy-
224	40.39	0.58	1,19-Eicosadiene
225	40.70	0.68	Cycloeicosane

be used in milk, cheese, and other fragrances (Sirois et al., 2018; Fechter-Leggett et al., 2018). It can also be used in cosmetic fresh fruit flavors and as gelatin hardener and photographic binder (Jedlicka et al., 2018).

Furan, 2-methyl-(1.75%) is used to produce vitamin B1, chloroquine phosphate, and promethazine phosphate (Carrasco et al., 2018). It is also a good solvent for the synthesis of pyrethroid pesticides and flavors and fragrances (Li et al., 2018). It is the raw material of allyl ketone, the pyrethroid and pyrethroid intermediate, while 2- methyl furan has anesthetic effects (Dohade and Dhepe, 2018).

Acetic acid (3.64%) can be used as acidifier, pickling agent, flavoring agent, spice (Spaepen et al., 2010), and is also a good antimicrobial agent, mainly attributed to its ability to reduce pH below the pH required for optimum microbial growth (Xie et al., 2018). Acetic acid is the earliest and most widely used sour agent in China (Kregiel et al., 2018). It is mainly used in compound seasoning, wax preparation, canned food, cheese, and jelly (Omoniyi and Dupont, 2018). The third generation of international beverage is made of vinegar as sour agent, supplemented by natural nutrition and health products (Chen et al., 2018; Philippe et al., 2018).

Propanoic acid (0.53%) is an important chemicals, and it is also the intermediate of many other fine chemicals (Bodulev et al., 2018). It is mainly used as food and feed additives, followed by home medicine, rare herbs, medicine, and spices (Belgrano et al., 2018; Nazareth et al., 2018). In terms of grain and feed additives, the application of propionic acid is significant and consumption is growing rapidly (Kim et al., 2018a, 2018b).

Toluene (0.82%) is widely used as a solvent and high octane gasoline additive, and is also an important raw material in the organic chemical industry (Chu et al., 2018; Xia et al., 2018). A series of intermediates derived from it are widely used in the production of fine chemicals such as dyes, pharmaceuticals, pesticides, propellants and explosives, additives, spices, and in the synthetic materials industry (Zhang et al., 2018a, 2018b; Liu et al., 2018a, 2018b).

n-Hexadecanoic acid (1.91%) has a special aroma and, and is a raw material for food additives such as fatty acid glycerides, fatty acid sorbitol anhydride esters, and sugar esters (Moreno et al., 2006). It is also the raw material for producing candles, soap, grease, softeners, and synthetic detergents (Song et al., 2008).

1-Octadecene (1.75%) is used in organic synthesis to produce surfactants, spices, palmites, dyes, and polymers (Pandey et al., 2018). Vanillin (0.95%) is a good perfume for obtaining powder and bean fragrance (Priefert et al., 2001). It can be widely used in almost all types of fragrance, such as violet, grass orchid, sunflower, and Oriental fragrance. It is also widely used in food such as vanilla bean, cream chocolate, toffee, flavoring biscuits, pastries, sweets and drinks, and tobacco flavors (Broadhurst and Jones, 2010). It is used in the analytical chemistry to test protein nitrophenylene, three benzene and tannic acid. In the pharmaceutical industry, it has uses in the production of hypotensive drugs methyl dopa, catechol drugs dopa, as well as betaine and dichlorfon (Frings et al., 1972).

Eugenol (0.48%) is the fragrance of the carnation flower, roses, and Xiang Wei (López de Lerma et al., 2018). It can be used as modifier and fixative. It can be perfused with colored perfumed soap, and is used in Xinxiang, Costus, Oriental and incense, and also in flavors such as spicy, peppermint, nuts, fruit flavors, dates and other tobacco flavors (Li et al., 2017). Eugenol also has a strong smell of *Dianthus odorus*, which is the blending basis of Kang and Zhi flavor, and is used in the blending of cosmetics, soap, food, and other flavors. As a local analgesic for dental caries, eugenol has strong bactericidal activity. Ding Zixiang phenol can also be used to produce isoniazid, a specific drug for treating tuberculosis (Wang et al., 2017).

2-Methoxy-4-vinylphenol (2.98%) and phenol, 4-ethyl-2-methoxy-(0.66%) are a food spice prescribed by GB 2760-1996, which can be used as food additives and fragrances (Xu et al., 2016). Catechols (1.22%) are important chemical intermediates, which are used in manufacture antioxidants, special inks, light stabilizers, rubber hardeners, plating additives, skin antiseptics, fungicides, hair dyes, photographic developers, and other important pharmaceutical intermediates (Kawahata et al., 2018). It is used to manufacture cough, butyl phenol, berberine, and isoproterenol (Roychoudhury et al., 2018). It can also be used for the production of 4-*tert*-butyl catechol as an inhibitor for styrene, butadiene and vinyl chloride (Yuzugullu Karakus et al., 2018).

Phenol, 2-methoxy-(1.98%) is mainly used to make coffee, vanilla, smoked tobacco and tobacco flavor (Hijas and Kumar, 2018; Zagorchev et al., 2018). It produces calcium guaiacol sulfonate in medicine, vanillin and artificial musk in perfume industry (Oliveira et al., 2018). P-Cresol (0.87%) is an intermediate for the production of antioxidant additive 2, 6-*tert*-butyl-4-methylphenol and P hydroxybenzaldehyde (Saito et al., 2018; Dou et al., 2004). It is also an important basic raw material for the production of Trimethylamine and the dye clenbuterol sulfonic acid. It is also an intermediate of the fungicide methyl paraquat, the insecticide Fenvalerate and ethermethrin (Muraleedharan et al., 2018; Liu et al., 2018a, 2018b). 1,3-Dioxol-2-one,4,5-dimethyl- (0.52%) can be used as an intermediate of olmesartan for antihypertensive drugs (Gao et al., 2018). Heptanoic acid (0.73%) are mainly used in the production of heptate esters as perfumes, safe glass polyvinyl butyral plasticizer esters, alkyd resin stabilizers can also be used as intermediates, as well as the production of polyol esters for synthetic lubricants (Coleman et al., 2018; Saren et al., 2018; Cui et al., 2017).

4. Conclusions and discussion

TGA in the bark of *Torreya grandis* can be divided into three stages: the first stage is mainly water evaporation, the second stage is caused by a small amount of polymer depolymerization and recombination, the third stage is mainly caused by the rapid decomposition of substances in the bark of *Torreya grandis* and a large number of volatile gases, resulting in weight loss.

The pyrolysis results showed that 205 substances were detected from 225 peaks. 1,3-Dioxol-2-one,4,5-dimethyl- can be used as an intermediate of olmesartan for antihypertensive drugs. 6-*tert*-Butyl-2,4-dimethylphenol acids can be used as antioxidants in polymeric resins and aviation fuels, and they are also very important pharmaceutical intermediates, as an inhibitor in MMA, UV

light-solid monomer, and resin and unsaturated resin, especially at high temperature. n-Hexadecanoic acid can be used as precipitating agents, chemical reagents and waterproofing agents, and are raw materials for making other food additives.

From the above studies, we can see that the effective components of Torreya bark have many functions, which are embodied in medicine, chemistry, food, and other aspects. Therefore, the bark of *Torreya grandis* is a resource with good application prospects, and has broad potential for sustainable utilization of forest biomass resources.

Acknowledgments

The authors acknowledge financial supported by the Scientific Innovation Fund for Graduate of Central South University of Forestry and Technology (20181012), Hunan Science Fund for Distinguished Young Scholars (16JJ1028), the Major Scientific and Technological Achievements Transformation Projects of Strategic Emerging Industries in Hunan Province (2016GK4045), and the Academician Reserve Personnel Training Plan of Lift Engineering Technical Personnel of Hunan Science and Technology Association (2017TJ-Y10).

References

Belgrano, F.D.S., Diegel, O., Pereira Jr., N., Hatti-Kaul, R., 2018. Cell immobilization on 3d-printed matrices: a model study on propionic acid fermentation. Bioresour. Technol. 249, 777.

Bodulev, O.L., Gribas, A.V., Sakharov, I.Y., 2018. Microplate chemiluminescent assay for hbv dna detection using 3-(10'-phenothiazinyl)propionic acid/n-morpholinopyridine pair as enhancer of hrp-catalyzed chemiluminescence. Anal. Biochem. 543, 33–36.

Broadhurst, R.B., Jones, W.T., 2010. Analysis of condensed tannins using acidified vanillin. J. Sci. Food Agric. 29 (9), 788–794.

Carrasco, E., Smith, K.J., Meloni, G., 2018. Synchrotron photoionization study of furan and 2-methylfuran reactions with methylidyne radical (ch) at 298 k. J. Phys. Chem. A 122 (1), 280–291.

Chen, B.Q., Cui, X.Y., Zhao, X., Zhang, Y.H., Piao, H.S., Kim, J.H., et al., 2006. Antioxidative and acute antiinflammatory effects of torreya grandis. Fitoterapia 77 (4), 262–267.

Chen, L., Zaipin, X.U., Zhang, C., Xiumei, W.U., Yulan, X.U., Chen, G., et al., 2018. Establishment of acute ulcerative colitis model induced by acetic acid in dog. China Animal Husbandry Veterin. Med.

Chu, F., Zheng, Y., Wen, B., Zhou, L., Yan, J., Chen, Y., 2018. Adsorption of toluene with water on zeolitic imidazolate framework-8/graphene oxide hybrid nanocomposites in a humid atmosphere. Rsc Adv. 8 (5).

Coleman, K.P., Grailer, T.P., Mcnamara, L.R., Rollins, B.L., Christiano, N.J., Kandárová, H., et al., 2018. Preparation of irritant polymer samples for an in vitro round robin study. Toxicol. In Vitro 50, 401.

Cui, D., Ebrahimi, M., Rosei, F., Macleod, J.M., 2017. Control of fullerene crystallization from 2d to 3d through combined solvent and template effects. J. Am. Chem. Soc. 139 (46), 16732–16740.

Debbarma, P., Zaidi, M.G.H., Kumar, S., Raghuwanshi, S., Yadav, A., Shouche, Y., Goel, R., 2018. Selection of potential bacterial strains to develop bacterial consortia for the remediation of e-waste and its in situ implications. Waste Manage. 79, 526–536.

Dohade, M.G., Dhepe, P.L., 2018. One pot conversion of furfural to 2-methylfuran in the presence of ptco bimetallic catalyst. Clean Technol. Environ. Policy 20 (4), 1–11.

Dou, L., Bertrand, E., Cerini, C., Faure, V., Sampol, J., Vanholder, R., et al., 2004. The uremic solutes p-cresol and indoxyl sulfate inhibit endothelial proliferation and wound repair. Kidney Int. 65 (2), 442–451.

Duan, M., Liu, Z.L., Yan, D.J., Peng, W.X., Baghban, A., 2018. Application of LSSVM algorithm for estimating higher heating value of biomass based on ultimate analysis. Energy Sources Part A-Recov. Utilizat. Environ. Effects 40 (6), 709–715.

Fang, S., Gu, W., Chen, L., Yu, Z., Dai, M., Lin, Y., et al., 2018. Ultrasonic pretreatment effects on the co-pyrolysis of municipal solid waste and paper sludge through orthogonal test. Bioresour. Technol. 258, 5–11.

Fechter-Leggett, E.D., White, S.K., Fedan, K.B., Cox-Ganser, J.M., Cummings, K.J., 2018. Burden of respiratory abnormalities in microwave popcorn and flavouring manufacturing workers. Occup. Environ. Med. 75 (10), 709–715.

Fedorovich, S.V., Voronina, P.P., Waseem, T.V., 2018. Ketogenic diet versus ketoacidosis: what determines the influence of ketone bodies on neurons? Neural Regen. Res. 13 (12), 2060–2063.

Francisco, R., Abreu, P.D., Plantz, B.A., Schlegel, V.L., Carvalho, R.A., Morais, P.V., 2011. Metal-induced phosphate extracellular nanoparticulate formation in ochrobactrum tritici 5bvl1. J. Hazard. Mater. 198, 31–39.

Frings, C.S., Fendley, T.W., Dunn, R.T., Queen, C.A., 1972. Improved determination of total serum lipids by the sulfo-phospho-vanillin reaction. Clin. Chem. 18 (7), 673–674.

Gao, M., Wang, J., Song, X., He, X., Dahlgren, R.A., Zhang, Z., et al., 2018. An effervescence-assisted switchable fatty acid-based microextraction with solidification of floating organic droplet for determination of fluoroquinolones and tetracyclines in seawater, sediment, and seafood. Anal. Bioanal. Chem.

Ge, S.B., Liu, Z.L., Furuta, Y., Peng, W.X., 2017. Adsorption characteristics of sulfur solution by acticarbon against drinking-water toxicosis. Saudi J. Biol. Sci. 24 (6), 1355–1360.

Hijas, K.M., Kumar, S.M., Byrappa, K., Geethakrishnan, T., Jeyaram, S., Nagalakshmi, R., 2018. Spectroscopic investigations using density functional theory on 2-methoxy- 4(phenyliminomethyl)phenol: a non linear optical material. J. Mol. Struct., 1155

Jedlicka, L.D.L., Silva, J.D.C., Balbino, A.M., Neto, G.B., Furtado, D.Z.S., Silva, H.D.T.D., et al., 2018. Effects of diacetyl flavoring exposure in mice metabolism. Biomed Res. Int., 1–11

Kastier, P., Krasylenko, Y.A., Martincova, M., Panteris, E., Samaj, J., Blehová, A., 2018. Cytoskeleton in the parasitic plant cuscuta during germination and prehaustorium formation. Front. Plant Sci. 9, 794.

Kawahata, M., Matsuura, M., Tominaga, M., Katagiri, K., Yamaguchi, K., 2018. Hydrogen-bonded structures from adamantane-based catechols. J. Mol. Struct. 1164, 116–122.

Kim, D.B., Jang, G.J., Yoo, M., Lee, G., Yun, S.S., Lim, H.S., et al., 2018a. Sorbic, benzoic and propionic acids in fishery products: a survey of the south korean market. Food Addit. Contam. Part A Chem. Anal. Control Exposure Risk Assess. 35 (6), 1071.

Kim, Y.M., Rhee, G.H., Ko, C.H., Kim, K.H., Jung, K.Y., Kim, J.M., et al., 2018b. Catalytic pyrolysis of pinus densiflora over mesoporous Al_2O_3 catalysts. J. Nanosci. Nanotechnol. 18 (9), 6300.

Kregiel, D., James, S.A., Rygala, A., Berlowska, J., Antolak, H., Pawlikowska, E., 2018. Consortia formed by yeasts and acetic acid Bacteriaasaia spp. in soft drinks. Antonie Van Leeuwenhoek 111 (3), 373–383.

Lans, A.M., Vodovotz, Y., 2018. Effect of galacto-oligosaccharide purity on water sorption and plasticization behavior. Food Chem. 268, 9–14.

Li, S., An, Y., Fu, W., Sun, X., Li, W., Li, T., 2017. Changes in anthocyanins and volatile components of purple sweet potato fermented alcoholic beverage during aging. Food Res. Int. 100 (Pt 2), 235–240.

Li, T., Hu, Y., Du, X., Tang, H., Shen, C., Wu, J., 2014. Salicylic acid alleviates the adverse effects of salt stress in torreya grandis, cv. merrillii seedlings by activating photosynthesis and enhancing antioxidant systems. Plos One 9 (10).

Li, Z., Ming, Z., Chen, X.R., Hua, M., 2018. Catalytic performance of Ni/Al2O3, catalyst for hydrogenation of 2-methylfuran to 2-methyltetrahydrofuran. J. Fuel Chem. Technol. 46 (1), 54–58.

Li, D.L., Wang, L.S., Peng, W.X., Ge, S.B., Li, N.C., Furuta, Y., 2015. Chemical structure of hemicellulosic polymers isolated from bamboo bio-composite during mold pressing. Polym. Compos. 38 (9), 2009–2015.

Lin, X., Zhang, Z., Zhang, Z., Sun, J., Wang, Q., Pittman, C.U., 2018. Catalytic fast pyrolysis of a wood-plastic composite with metal oxides as catalysts. Waste Manage. 79, 38–47.

Liu, Z., 2018. Economic analysis of energy production from coal/biomass upgrading; Part 1: hydrogen production. Energy Source Part B 13 (2), 132–136.

Liu, W.C., Tomino, Y., Lu, K.C., 2018a. Impacts of indoxyl sulfate and p-cresol sulfate on chronic kidney disease and mitigating effects of AST-120. Toxins (Basel) 10 (9).

Liu, X.K., Zhang, X.L., Qian, L., Xiang, L.I., 2018b. Determination and correlation of liquid equilibrium of the n-dodecane-toluene-phenol ternary system. J. Chem. Eng. Chinese Univ. 32 (2), 275–279.

López de Lerma, N., Peinado, R.A., Puigpujol, A., Mauricio, J.C., Moreno, J., GarcíaMartínez, Teresa, 2018. Influence of two yeast strains in free, bioimmobilized or immobilized with alginate forms on the aromatic profile of long aged sparkling wines. Food Chem. 250 (1), 22–29.

Mehrabian, H., Rosa, M.D., Haider, M.A., Martel, A.L., 2015. Pharmacokinetic analysis of prostate cancer using independent component analysis. Magn. Reson. Imaging 33 (10), 1236–1245.

Moreno, E., Cordobilla, R., Calvet, T., Lahoz, F.J., Balana, A.I., 2006. The c form of n-hexadecanoic acid. Acta Crystallogr. 62 (3), o129–o131.

Muraleedharan, L., Bellundagere, Chandrashekara, M., Prakash, S.J., Yajnavalkya, et al., 2018. Clay-based solid acid catalyst for the alkylation of p-cresol with tert-butyl alcohol. Chemistryselect 3 (2), 801–808.

Nazareth, T.C., De, A.O.P., Ramos, L.R., Silva, E.L., 2018. Valorization of the crude glycerol for propionic acid production using an anaerobic fluidized bed reactor with grounded tires as support material. Appl. Biochem. Biotechnol. (1), 1–14

Ni, L., Shi, W.Y., 2014. Composition and free radical scavenging activity of kernel oil from torreya grandis, carya cathayensis, and myrica r ubra. Iranian J. Pharm. Res. IJPR 13 (1), 221.

Okamoto, S., Honda, T., Miyakoshi, T., Han, B., Sablier, M., 2018. Application of pyrolysis-comprehensive gas chromatography/mass spectrometry for identification of asian lacquers. Talanta 189, 315–323.

Oliveira, L., Souzasilva, F., De, L.C.C., Cysnefinkelstein, L., De, M.S.P., De, F.O.J., et al., 2018. Antileishmanial activity of 2-methoxy-4h-spiro-[naphthalene-1,2'-oxiran]-4-one (epoxymethoxy-lawsone): a promising new drug candidate for leishmaniasis treatment. Molecules 23 (4), 864.

Omoniyi, O.A., Dupont, V., 2018. Chemical looping steam reforming of acetic acid in a packed bed reactor. Appl. Catal. B Environ. 226, 258–268.

Pandey, S., Raj, K.V., Shinde, D.R., Vanka, K., Kashyap, V., Kurungot, S., et al., 2018. Iron catalyzed hydroformylation of alkenes under mild conditions: evidence of an fe(ii) catalyzed process. J. Am. Chem. Soc. 140 (12), 4430–4439.
Peng, W.X., Lin, Z., Wang, L., Chang, J., Gu, F., Zhu, X., 2016a. Molecular characteristics of illicium verum extractives to activate acquired immune response. Saudi J. Biol. Sci. 23 (3), 348.
Peng, W.X., Liu, Z., Motaharinezhad, M., Banisaeed, M., Shahraki, S., Beheshti, M., et al., 2016b. A detailed study of oxy-fuel combustion of biomass in a circulating fluidized bed (cfb) combustor: evaluation of catalytic performance of metal nanoparticles (al, ni) for combustion efficiency improvement. Energy 109, 1139–1147.
Peng, W.X., Ge, S.B., Ebadi, A.G., Hisoriev, H., Esfahani, M.J., 2017. Syngas production by catalytic co-gasification of coal-biomass blends in a circulating fluidized bed gasifier. J. Clean. Prod. 168, 1513–1517.
Philippe, C., Krupovic, M., Jaomanjaka, F., Claisse, O., Petrel, M., Marrec, C.L., 2018. Bacteriophage gc1, a novel tectivirus infectinggluconobacter cerinus, an acetic acid bacterium associated with wine-making. Viruses 10 (1), 39.
Priefert, H., Rabenhorst, J., Steinbüchel, A., 2001. Biotechnological production of vanillin. Appl. Microbiol. Biotechnol. 56 (3–4), 296–314.
Raba, D.N., Chambre, D.R., Copolovici, D.M., Moldovan, C., Copolovici, L.O., 2018. The influence of high-temperature heating on composition and thermo-oxidative stability of the oil extracted from arabica coffee beans. Plos One 13 (7), e0200314.
Roychoudhury, A., Basu, S., Jha, S.K., 2018. Surface functionalized prussian blue-coated nanostructured nickel oxide as a new biosensor platform for catechol detection. Anal. Sci. 34 (10), 1163–1169.
Saeed, M.K., Deng, Y., Dai, R., Li, W., Yu, Y., Iqbal, Z., 2010. Appraisal of antinociceptive and anti-inflammatory potential of extract and fractions from the leaves of torreya grandis fort ex. lindl. J. Ethnopharmacol. 127 (2).
Saito, Y., Sato, T., Tsuji, H., Nomoto, K., 2018. Identification of phenol-and p-cresol-producing intestinal bacteria by using media supplemented with tyrosine and its metabolites. FEMS Microbiol. Ecol. 94 (9), 1–11.
Saren, G., Yi, X., Gong, Y., 2018. Pleiotropic effects and biological activities of atorvastatin: the sun never set. Int. J. Cardiol. 254, 261.
Shi, H., Wang, H., Wang, M., Li, X., 2009. Antioxidant activity and chemical composition of torreya grandis cv. merrillii seed. Nat. Prod. Commun. 4 (11), 1565–1570.
Sirois, J.J., Padgitt-Cobb, L., Gallegos, M.A., Beckman, J.S., Beaudry, C.M., Hurst, J.K., 2018. Oxidative release of copper from pharmacologic copper bis (thiosemicarbazonato) compounds. Inorganic Chem. 57 (15), 8923–8932.
Song, Y., Yao, Y., Chen, C., Cui, K., Wang, L., 2008. Structural investigation of n -hexadecanoic acid multilayers on mica surface: atomic force microscopy study. Appl. Surf. Sci. 254 (11), 3306–3312.
Spaepen, S., Vanderleyden, J., Remans, R., 2010. Indole-3-acetic acid in microbial and microorganism-plant signaling. FEMS Microbiol. Rev. 31 (4), 425–448.
Vielhauer, O., Zakhartsev, M., Horn, T., Takors, R., Reuss, M., 2011. Simplified absolute metabolite quantification by gas chromatography–isotope dilution mass spectrometry on the basis of commercially available source material. J. Chromatogr. B Anal. Technol. Biomed Life Sci. 879 (32), 3859–3870.
Wang, L.S., Ge, S.B., Liu, Z.L., Zhou, Y.F., Yang, X.X., Yang, W., Li, D.L., Peng, W.X., 2018. Properties of antibacterial bioboard from bamboo macromolecule by hot press. Saudi J. Biol. Sci. 25 (3), 465–468.
Wang, J., Huang, Y., Fang, M., Zhang, Y., Zheng, Z., Zhao, Y., et al., 2002. Brefeldin a, a cytotoxin produced by paecilomyces sp. and aspergillus clavatus isolated from taxus mairei and torreya grandis. Pathogens Dis. 34 (1), 51–57.
Wang, P., Wu, Q., Jiang, X., Wang, Z., Tang, J., Xu, Y., 2017. Bacillus licheniformis affects the microbial community and metabolic profile in the spontaneous fermentation of daqu starter for chinese liquor making. Int. J. Food Microbiol. 250, 59–67.
Wu, X., Ba, Y., Wang, X., Niu, M., Fang, K., 2018. Evolved gas analysis and slow pyrolysis mechanism of bamboo by thermogravimetric analysis, Fourier transform infrared spectroscopy and gas chromatography-mass spectrometry. Bioresour. Technol. 266, 407–412.
Xia, D., Xu, W., Hu, L., He, C., Leung, D.Y.C., Wang, W., et al., 2018. Synergistically catalytic oxidation of toluene over mn modified g-c 3 n 4 /zsm-4 under vacuum uv irradiation. J. Hazard. Mater. 349, 91–100.
Xie, A.D., Cong-Jun, L.I., Liu, K.Z., Qing, H.U., 2018. Study on the acetic acid fermentation technology of osmanthus and jujube fruit vinegar. China Condiment.
Xu, J., Tahmasebi, A., Yu, J., 2016. An experimental study on the formation of methoxyaromatics during pyrolysis of eucalyptus pulverulenta: yields and mechanisms. Bioresour. Technol. 218, 743–750.
Yang, C., Hu, R., Li, Q., Li, S., Xiang, J., Guo, X., Wang, S., Zeng, Y., Li, Y., Yang, G., 2018. Visualization of parallel G-quadruplexes in cells with a series of new developed bis(4-aminobenzylidene)acetone derivatives. ACS Omega 3 (9), 10487–10492.
Yuzugullu Karakus, Y., Goc, G., Balci, S., Yorke, B.A., Trinh, C.H., McPherson, M.J., Pearson, A.R., 2018. Identification of the site of oxidase substrate binding in Scytalidium thermophilum catalase.
Zagorchev, L., Albanova, I., Tosheva, A., Li, J., Teofanova, D., 2018. Salinity effect on Cuscuta campestris Yunck. Parasitism on Arabidopsis thaliana L. Plant Physiol. Biochem. 132, 408–414.
Zeng, Y., Ye, S., Yu, W., Wu, S., Hou, W., Wu, R., et al., 2014. Genetic linkage map construction and qtl identification of juvenile growth traits in torreya grandis. BMC Genet. 15 (S1), 1–9.
Zhang, C., Huang, H., Li, G., Wang, L., Song, L., Li, X., 2018a. Zeolitic acidity as a promoter for the catalytic oxidation of toluene over mno x/hzsm-5 catalysts. Catal. Today. S0920586118302475.
Zhang, Y.H., Liu, C.Y., Jiu, B.B., Liu, Y., Gong, F.L., 2018b. Facile synthesis of pd-decorated zno nanoparticles for acetone sensors with enhanced performance. Res. Chem. Intermed. 44 (3), 1569–1578.
Zhu, X., Dong, L., Jiang, L., Li, H., Sun, L., Zhang, H., et al., 2015. Constructing a linkage-linkage disequilibrium map using dominant-segregating markers. DNA Res. 23 (1), 1–10.
Zong, H., Cao, Y., Liu, Z., 2018. Energy security in group of seven (g7): a quantitative approach for renewable energy policy. Energy Source Part B 13 (3), 173–175.